

# Exploring Multi-Component Superconducting Compounds by a High-Pressure Method and Ceramic Combinatorial Chemistry

N. D. Zhigadlo<sup>1</sup> · M. Iranmanesh<sup>1</sup> · W. Assenmacher<sup>2</sup> · W. Mader<sup>2</sup> · J. Hulliger<sup>1</sup>

Received: 3 September 2016 / Accepted: 7 September 2016  
© Springer Science+Business Media New York 2016

**Abstract** In this short review, we provide some new insights into the material synthesis and characterization of modern multi-component superconducting oxides. Two different approaches such as the high-pressure, high-temperature method and ceramic combinatorial chemistry will be reported with application to several typical examples. First, we highlight the key role of the extreme conditions in the growth of Fe-based superconductors, where a careful control of the composition-structure relation is vital for understanding the microscopic physics. The availability of high-quality  $LnFeAsO$  ( $Ln$  = lanthanide) single crystals with substitution of O by F, Sm by Th, Fe by Co, and As by P allowed us to measure intrinsic and anisotropic superconducting properties such as  $H_{c2}$ ,  $J_c$ . Furthermore, we demonstrate that combinatorial ceramic chemistry is an efficient way to search for new superconducting compounds. A single-sample synthesis concept based on multi-element ceramic mixtures can produce a variety of local products. Such a system needs local probe analyses and separation techniques to identify compounds of interest. We present the results obtained from random mixtures of Ca, Sr, Ba, La, Zr, Pb, Tl, Y, Bi, and Cu oxides reacted at different conditions. By adding Zr but removing Tl, Y, and Bi, the bulk state superconductivity got enhanced up to about 122 K.

**Keywords** Superconductors · High-pressure synthesis · Ceramic combinatorial chemistry

Iron-based superconductors are known to exhibit many unique properties in their superconducting and normal states, some of which are still open to investigation. Besides high critical temperatures, these materials have some similarities and differences compared to cuprate superconductors, which raised the question about the superconductivity mechanism [1]. In all members of the so-called  $Ln1111$ - $LnFePnO$  family ( $Ln$ : lanthanide,  $Pn$ : pnictogen), the  $Fe_2Pn_2$  layer is essential for superconductivity while the  $Ln_2O_2$  layer plays a role of a charge-carrier source. A distinctive feature of this family is that the charge-carrier density and thus the electronic properties can be changed through chemical substitution at every atomic site [2–7]. Electron doping can be realized by the partial substitutions of F or H for O as well as by oxygen deficiency. In addition to the charge-carrier doping in  $Ln_2O_2$  layers, the partial substitution of Fe with Co or Ni also leads to superconductivity. Besides, the carrier concentration structural parameters play also an important role for obtaining high  $T_c$ s. Further progress in exploring the physical properties of  $Ln1111$  superconductors depends crucially on the availability of sufficiently large single crystals of high quality. High-pressure and high-temperature technique yields quite promising results, and during the last few years,  $Ln1111$  crystals with substitutions on various sites were produced [2–7]. This method has several advantages in comparison with the conventional ampoule method, since it avoids vaporization losses of volatile components and allows control of the composition and doping event at high temperatures required for single-crystal growth. Fluxes, such as NaCl/KCl, NaAs, and KAs, yielded most successful results

✉ N. D. Zhigadlo  
nzhigadlo@gmail.com

<sup>1</sup> Department of Chemistry and Biochemistry, University of Bern, 3012 Bern, Switzerland

<sup>2</sup> Institute of Inorganic Chemistry, University of Bonn, 53117 Bonn, Germany

[2, 3, 6]. Table 1 provides the list of  $Ln1111$  crystals grown at the high-pressure and high-temperature conditions. X-ray structural investigations confirmed good structural quality and show modifications due to substitutions, which are linked to superconducting properties. A sufficiently large size of crystals promotes the development of single-crystal experimental techniques previously not possible for  $Ln1111$ -type pnictides. Most outstanding results obtained in the last few years are presented below.

In particular, the application potential of  $Ln1111$  system is rather high since it produces not only very high critical fields exceeding 50 T at liquid He temperatures but also high critical current densities [8]. Both these properties show a tendency towards isotropic behavior at low temperatures. It was demonstrated that by introducing a low density of correlated nano-scale defects into  $SmFeAs(O,F)$  crystals by heavy-ion irradiation, one can increase its critical current density to up to  $2 \times 10^7$  A/cm<sup>2</sup> at 5 K, the highest ever reported for an iron-based superconductor without reducing its critical temperature of 50 K [9]. Recent progress in  $SmFeAsO_{1-x}F_x$  thin-film synthesis has provided the promise for fabricating high-quality films [10]. In this respect,  $SmFeAsO_{1-x}F_x$ -based superconducting products with performance comparable to the state-of-the-art of cuprates can be expected. For possible application of Fe-based superconductors, it is highly desirable to explore the nature of the vortices and their interaction with the pinning landscape. Recently, the authors of refs. [11, 12] have

observed a distinct change in the nature of the vortices from well-pinned slow-moving Abrikosov-like to weakly pinned fast-flowing Josephson-like in the  $SmFeAsO_{1-x}F_x$  with  $T_c \sim 48$ –50 K on cooling below a temperature  $T^* \sim 41$ –42 K. The existence of such a vortex state is the result of a delicate balance between the properties of the material, such as the coherence length and the interlayer separation. This vortex dynamics could become technologically relevant as superconducting applications will always operate deep in the Josephson regime. Recently, angle-resolved photoemission spectroscopy (ARPES) has been used to investigate the inherent electronic structure of the  $Sm(Fe,Co)AsO$  ( $T_c = 16$  K) and the  $NdFeAsO_{0.6}F_{0.4}$  ( $T_c = 38$  K) crystals [13–15]. It was demonstrated that the enhancement of superconductivity in  $Ln1111$  family correlates closely with the fine-tuning of one of the band-edge singularities to within a fraction of the superconducting energy gap  $\Delta$  below the Fermi level. These results provide completing evidence that the band-structure singularities near the Fermi level in the Fe-based superconductors must be explicitly accounted in any attempt to understand the mechanism of superconducting pairing in these materials.

The structure of the  $Ln1111$  iron pnictide superconductors is made of a superlattice of FeAs layers intercalated by spacer oxide layers like  $LnO_{1-x}F_x$  or  $LnO_{1-x}$ , i.e., they represent practical realization of a heterostructure at the atomic limit, which was described to be the essential material architecture for the emergence of high  $T_c$  superconductivity. The

**Table 1** Structural and superconducting properties of  $LnFeAsO$  ( $Ln = Sm, Nd, Pr$ ) single crystals

Composition	Lattice units (Å)	$h_{Pn}$	$H//ab$	$H//c$	$J_c$ (A/cm <sup>2</sup> )	$T_c$ (K)	Ref.
SmFeAsO	$a = 3.9427(1)$ $c = 8.4923(3)$	1.3613(9)					[2]
SmFeAsO <sub>0.86-x</sub> F <sub>x</sub>	$a = 3.9390(10)$ $c = 8.4684(6)$				$\sim 2 \times 10^6$	48	[2, 8]
SmFeAsO <sub>0.85</sub> F <sub>0.15</sub>			(Pb ions irradi.)		$\sim 2 \times 10^7$	50	[9]
Sm <sub>0.89</sub> Th <sub>0.11</sub> FeAsO	$a = 3.9369(1)$ $c = 8.4510(6)$	1.3615(9)	$\sim 5.4$	$\sim 2.7$	$\sim 8 \times 10^5$	49.5	[4]
SmFeAs <sub>0.5</sub> P <sub>0.5</sub> O <sub>0.85</sub>	$a = 3.911022(8)$ $c = 8.3367(2)$	1.293(2)	$\sim 5.7$	$\sim 1.3$		21.7	[5]
SmFe <sub>0.92</sub> Co <sub>0.08</sub> AsO	$a = 3.9410(2)$ $c = 8.4675(7)$	1.3489(9)	$\sim 8.7$	$\sim 1.7$	$\sim 10^6$	16.4	[6]
NdFeAsO <sub>0.65</sub> F <sub>0.35</sub>	$a = 3.9629(6)$ $c = 8.5493(17)$	1.353(2)				38.5	[6]
NdFeAsO <sub>0.75</sub> F <sub>0.25</sub>	$a = 3.9643(6)$ $c = 8.5423(14)$	1.356(4)				19	[6]
PrFeAsO <sub>0.7</sub> F <sub>0.3</sub>					$\sim 10^6$	25.2	[6]

$h_{Pn}$  is the height of the As/P atoms above the plane of iron atoms. The upper critical field  $H_{c2}$  slopes, for  $H$  oriented parallel ( $H//ab$ ) and perpendicular ( $H//c$ ) to the  $ab$  plane. The critical current density  $J_c$  estimated at 2–5 K. The critical temperature  $T_c$  obtained from the resistivity and/or magnetic measurements

critical temperature  $T_c$  is controlled by both charge density and lattice effects [16, 17]. One of the intriguing points is the future perspectives to synthesize new materials containing both FeAs and CuO<sub>2</sub> superconducting layers. In such materials, the proximity effect between two types of layers with different pairing symmetries can result in interesting novel phenomena [18, 19].

Throughout history, material scientists have relied on the slow trial-and-error process for discovering and developing new materials. In contrast, an attractive theme in modern material science is the idea of knowledge-based design of new materials [20, 21]. Pioneered by pharmaceutical industry and adopted for the purposes of materials science, the combinatorial solid-state approach represents today an important tool in the development and optimization of materials. Thousands of compositionally varying samples may be synthesized, processed, and screened in a single experiment. Consequently, new innovative and high-risk projects are needed for a further exploration of this field.

In our previous work, we studied the non-stoichiometric combination of nine elements (P0, see Table 2) providing high-temperature superconducting phases showing a bulk  $T_c$  up to 115 K [21]. To understand the origin of SC phase/s, eliminating different elements was undertaken (Table 2) to explore the effect of each element on  $T_c$ . Removing elements like Sr, Ca, La, and Ba showed to be crucial for high  $T_c$ s while other elements such as Y, Pb, Bi, and Tl did not have a significant impact. Consequently, samples (P1) were prepared without Tl, Bi, and Y for which SQUID results indicate the possibility to produce SC at  $T_c \approx 95$  K. This is of interest because many of these remaining compositions must be reacted at high pressure to produce SC compounds [22–26].

The synthesis of this kind of library was performed by ceramic reactions as reported recently [21]. We prepared several initial compositions by reacting different combinations and compositions of oxides, peroxides and carbonates, i.e., 2 BaO<sub>2</sub>, 2 CaCO<sub>3</sub>, 2 SrCO<sub>3</sub>, 0.25 La<sub>2</sub>O<sub>3</sub>, 0.1 PbCO<sub>3</sub>, 0.5 ZrO<sub>2</sub>, and 4.5 CuO. Molar ratios of these materials were mixed in a ball-mill and then pressed into pellets. Calcination was performed by raising the temperature just below the formation of liquids (around 930 °C), followed by a 10 °C/h temperature descent for 13 h to 800 °C. The heat treatment was performed under O<sub>2</sub> gas flow at normal pressure. The obtained samples were grind in a mortar and SC grains were

isolated by magnetic separation [27]. The DC magnetic susceptibility of single grains and bulk samples were measured by SQUID magnetometry.

For further synthesis, we considered adding other elements such as Al, Zr, Gd, In, and Sn to the most promising initial mixtures (P0 and P1). The results from SQUID measurements showed that 1 molar ratio of ZrO<sub>2</sub> was sufficient to improve the  $T_c$  from 115 to 121 K (sample P0), whereas addition of other elements did not improve results. Interestingly, adding ZrO<sub>2</sub> to P1,  $T_c$  increased from 95 to 122 K. Addition of Zr combined with Pb in sample P2 increased thermodynamically the stability and reproducibility of high  $T_c$  SC phases. These results support that Zr and Pb can promote the reaction for Sr, La, Ba, Ca, and Cu (P1) samples. However, no report on a high-temperature superconductor compounds containing Zr (constitutional, not just doping) could be found in literature. This lead to the conclusion that only a small amount of Zr will promote the reaction and most likely ZrO<sub>2</sub> is not a constitutional element for the superconducting phases. It could be that ZrO<sub>2</sub> is trapping some component and this is promoting the SC phase formation at normal pressure.

Looking through the meanwhile long list of structural types and compositions [22–26], we can notice that superconductivity of a  $T_c$  of 110–117 K can be established simply by elements such as Ca, Sr, Ba, and Cu (Sr<sub>3</sub>Cu<sub>2</sub>O<sub>5+ $\delta$</sub>  (100 K) [22], Sr<sub>4</sub>Cu<sub>3</sub>O<sub>8</sub> (100 K) [23], Sr<sub>0.63</sub>Ca<sub>0.27</sub>CuO<sub>2</sub> (110 K) [24], Sr<sub>2</sub>CaCu<sub>2</sub>O<sub>5.6</sub> (109 K) [25], Ba-Ca-Cu-O (117 K) [26]). However, all known reports on these compositions use high-pressure methods for the synthesis. As shown, we demonstrate superconductivity up to about 122 K in the system containing Ca, Sr, Ba, Cu, La, Pb, and Zr. Thus, besides the key superconducting elements such as Ca, Sr, Ba, and Cu, the minor La, Zr, and Pb components may drive the mechanism of formation of high  $T_c$  superconducting phase/s.

One of the know system that can produce such high  $T_c$  from abovementioned elements is the Pb-Sr-Ca-Cu-O [28–30]. By using high-pressure method, Tamura et al. [28] have succeeded in synthesizing Pb-1223 phase with composition of Pb<sub>0.5</sub>Sr<sub>2.8</sub>Ca<sub>1.7</sub>Cu<sub>3.0</sub>O<sub>y</sub> and  $T_c$  of about 120 K. Transmission electron microscopy investigations revealed the formation of a Pb-12(n-1)n homologous series in these layered cuprates and the Pb-1223 phase showed formation of a superlattice with the following composition:

**Table 2** Compositions of the initial mixtures

	Y <sub>2</sub> O <sub>3</sub>	BaO <sub>2</sub>	CaCO <sub>3</sub>	Bi <sub>2</sub> O <sub>3</sub>	SrCO <sub>3</sub>	La <sub>2</sub> O <sub>3</sub>	Tl <sub>2</sub> O <sub>3</sub>	PbCO <sub>3</sub>	ZrO <sub>2</sub>	CuO	$T_c$ (K)
P0	0.5	4	4	1	4	0.5	4	0.2	–	9	115
P1	–	4	4	–	4	0.5	–	0.2	–	9	95
P2	–	4	4	–	4	0.5	–	0.2	1	9	122

( $\text{Pb}_{0.5}\text{Sr}_{0.2}\text{Cu}_{0.3}\text{Sr}_2(\text{Ca}_{1.7}\text{Sr}_{0.3})\text{Cu}_3\text{O}_y$  [29]. We note that delicate control of oxygen content is required in order to obtain high  $T_c$ s in these Pb-based high-pressure prepared phases [28–30]. A natural question is raised if such kind of phases can appear at ambient pressure. Rouillon et al. [31] reported a weak Meissner signal (2–3 %) above 100 K in their Pb-Sr-Y-Ca-Cu-O samples prepared by an encapsulation technique using quartz ampules. Obviously, there are conditions that the Pb-1223 phase can be made without high-pressure techniques.

We performed all our synthesis experiments according to the molar ratios represented in Table 2. While the synthesis was done under oxygen-flowing atmosphere, no special attention was given to control the oxygen content from starting compositions. Figure 1 shows typical temperature dependence of the magnetic susceptibility measured on P2 “SrCaBaCuPbLaZrO” polycrystalline sample. The onset of the superconducting transition up to 122 K (in some grains up to 127 K) was revealed for many measured pieces. Relatively high diamagnetic shielding at 1.8 K supports bulk superconductivity, while the overall transition is quite broad, thus reflecting inhomogeneity.

Figure 2 shows representative SEM images of a combinatorial P2 sample. The morphology of particles is plate-like and crystalline but particles are intergrown. The grains representing a uniform sub-micrometer size distribution show coalescence that it promoted by thermal treatment. The composition of as-synthesized P2 samples was investigated by EDX. Four to six wide-area spots were analyzed in that sample showing  $T_c$  of 122 K. By normalizing the EDX data to 3 Cu atoms, we observe the following composition:

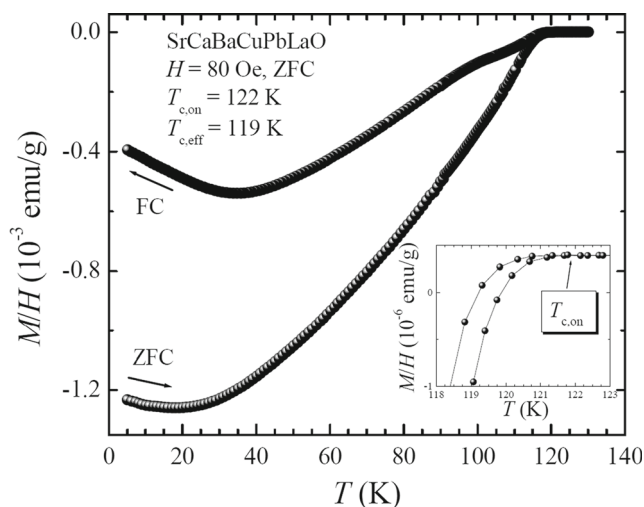


**Fig. 1** Temperature dependence of the magnetic susceptibility measured on SrCaBaCuPbLaO polycrystalline sample with  $T_{c,on}$  of 122 K in an applied field of 80 Oe. ZFC zero-field-cooling, FC field-cooling curves

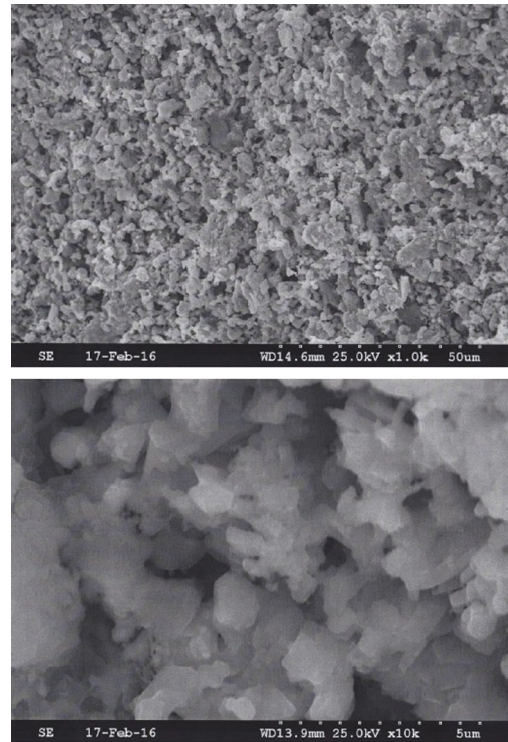


**Fig. 2** SEM images of a combinatorial sample. The morphology of the particles is plate-like and crystalline but particles are intergrown. The grains representing a uniform sub-micrometer size distribution show coalescence that is promoted by thermal treatment

( $\text{Pb}_{0.21}\text{Sr}_{2.85}\text{Ca}_{1.8}\text{Cu}_3\text{O}_y$ )( $\text{La}_{0.26}\text{Ba}_{1.13}\text{Zr}_{0.62}$ ). Surprisingly, in some part, the composition of the high-pressure Pb-1223 phase was also present, but with substantial lower concentration of Pb atoms. While other elements such as La and Zr are present, it is not clear if they are incorporated in the phase.

In order to get more information about the composition of the superconducting phase our magnetic separation technique played a key role [27]. We have been able to capture a considerable number of SC grains, which are attached perpendicular to a magnetized wire, to deposit them in a small container (shown in the left panel of Fig. 3). The size of captured grains varies between 60 and 300  $\mu\text{m}$ , and the overall morphology was comparable to that of presented in Fig. 2. Scanning SQUID microscopy measurements on captured grains confirmed their high  $T_c$ s ( $\sim 120$  K). A subsequent preliminary elemental analysis attempt has been done by EDS spot analysis (5 nm diameter) on small pieces of grains using a transmission electron microscopy (FEI CM300UT-FEG) in scanning mode (right panel of Fig. 3). These crystals differ strongly in their composition and also from the composition of the entire matrix. However, not all of the cations from the starting mixture can be found in each of the crystals. By performing analyses at randomly selected areas and looking close at the elemental composition and



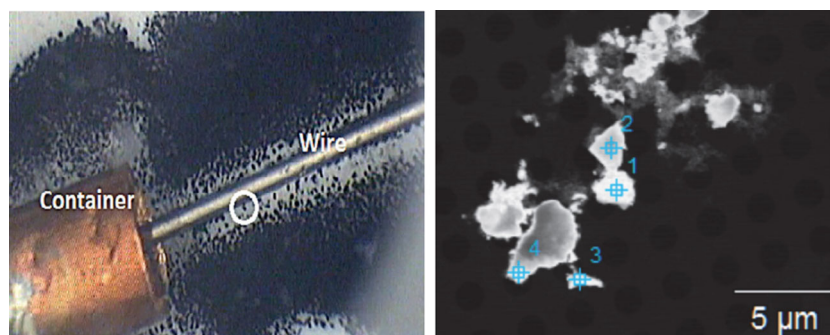


**Fig. 3** *Left panel:* Demonstration of the capturing of superconducting particles by magnetic separation, perpendicular to a magnetized iron wire (AC field of 50 Hz and ZFC, YBCO sample), moved into

a container. *Right panel:* STEM HAADF image of grinded superconducting crystals obtained by ceramic combinatorial synthesis and used for EDX spot analyses

atomic percentages of spots, we anticipate that the dominant superconducting compound is basically made from Sr, Ba, Ca, and Cu elements, and the amount of La and Pb is minimal and not present in every grain. A further analysis is underway identifying the phases and chemical formula to the best of present means.

In summary, we present a short overview of  $\text{LnFeAsO}$  single crystals grown by high-pressure technique. The availability of  $\text{Ln1111}$  single crystals made it possible to determine several superconducting parameters and their anisotropy. The upper critical fields and critical current densities are very high for these crystals which open up a way for future applications. Combinatorial chemistry using inhomogeneous ceramic samples made up of several elements has produced an interesting result in the phase system of Ca-Sr-Ba-Cu when adding  $\text{ZrO}_2$  and  $\text{PbO}$ . Bulk susceptibility SQUID measurements could demonstrate superconductivity up to 122 K. In this phase system, known superconducting phases were so far only obtained under *high pressure* conditions. The EDX analysis on some grains support compounds mainly made of Ca, Sr, Ba, and Cu and possibly containing a small amount of La and Pb. However, a combined instrumental, i.e., low-temperature electron microscopy and scanning squid microscopy would be required to explore libraries forming in such single ceramic samples. This is of interest because high-temperature cuprates up to 122 K do not represent frequent materials appearing in conventional syntheses containing no Tl, Bi, and Hg.

## References

- Campi, G., Bianconi, A., Poccia, N., Bianconi, G., Barda, L., Arrighetti, G., Innocenti, D., Karpinski, J., Zhigadlo, N.D., Kazakov, S.M., Burghammer, M., Zimmermann, M.v., Sprung, M., Ricci, A.: *Nature* **525**, 359 (2015)
- Zhigadlo, N.D., Katrych, S., Bukowski, Z., Weyneth, S., Puzniak, R., Karpinski, J.: *J. Phys.: Condens. Matter* **20**, 342202 (2008)
- Karpinski, J., Zhigadlo, N.D., Katrych, S., Bukowski, Z., Moll, P., Weyneth, S., Keller, H., Puzniak, R., Tortello, M., Daghero, D., Gonnelli, R., Maggio-Aprile, I., Fasano, Y., Fischer, Ø., Rogacki, K., Batlogg, B.: *Physica C* **469**, 370 (2009)
- Zhigadlo, N.D., Katrych, S., Weyneth, S., Puzniak, R., Moll, P.J.W., Bukowski, Z., Karpinski, J., Keller, H., Batlogg, B.: *Phys. Rev. B* **82**, 064517 (2010)
- Zhigadlo, N.D., Katrych, S., Bendele, M., Moll, P.J.W., Tortello, M., Weyneth, S., Pomjakushin, V.Y., Kanter, J., Puzniak, R., Bukowski, Z., Keller, H., Gonnelli, R.S., Khasanov, R., Karpinski, J., Batlogg, B.: *Phys. Rev. B* **84**, 134526 (2011)
- Zhigadlo, N.D., Weyneth, S., Katrych, S., Moll, P.J.W., Rogacki, K., Bosma, S., Puzniak, R., Karpinski, J., Batlogg, B.: *Phys. Rev. B* **86**, 214509 (2012)
- Zhigadlo, N.D.: *J. Cryst. Growth* **382**, 75 (2013)
- Moll, P.J.W., Puzniak, R., Balakirev, F., Rogacki, K., Karpinski, J., Zhigadlo, N.D., Batlogg, B.: *Nat. Mater* **9**, 628 (2010)
- Fang, L., Jia, Y., Mishra, V., Chaparro, C., Vlasko-Vlasov, V.K., Koshelev, A.E., Welp, U., Crabtree, G.W., Zhu, S., Zhigadlo, N.D., Katrych, S., Karpinski, J., Kwok, W.K.: *Nat. Commun.* **4**, 2655 (2013)
- Iida, K., Hänisch, J., Tarantini, C., Kurth, F., Jaroszynski, J., Ueda, S., Naito, M., Ichinose, A., Tsukada, I., Reich, E., Grinenko, V., Schultz, L., Holzappel, B.: *Sci. Rep.* **3**, 2139 (2013)
- Moll, P.J.W., Balicas, L., Geshkenbein, V., Blatter, G., Karpinski, J., Zhigadlo, N.D., Batlogg, B.: *Nat. Mater* **12**, 134 (2013)
- Moll, P.J.W., Balicas, L., Zhu, X., Wen, H.-H., Zhigadlo, N.D., Karpinski, J., Batlogg, B.: *Phys. Rev. Lett.* **113**, 186402 (2014)
- Charnukha, A., Thirupathaiah, S., Zabolotnyy, V.B., Büchner, B., Zhigadlo, N.D., Batlogg, B., Borisenko, S.V.: *Sci. Rep.* **5**, 10392 (2015)
- Charnukha, A., Evtushinsky, D.V., Matt, C.E., Xu, N., Shi, M., Büchner, B., Zhigadlo, N.D., Batlogg, B., Borisenko, S.V.: *Sci. Rep.* **5**, 18273 (2015)
- Borisenko, S.V., Evtushinsky, D.V., Liu, Z.-H., Morozov, I., Kappenberger, R., Wurmehl, S., Büchner, B., Yaresko, A.N., Kim, T.K., Hoesch, M., Wolf, T., Zhigadlo, N.D.: *Nat. Phys.* **12**, 311 (2016)
- Ricci, A., Poccia, N., Ciasca, G., Fratini, M., Bianconi, A.: *J. Supercond. Nov. Magn.* **22**, 589 (2009)
- Ricci, A., Poccia, N., Joseph, B., Barba, L., Arrighetti, G., Ciasca, G., Yan, J.-Q., McCallum, R.W., Lograsso, T.A., Zhigadlo, N.D., Karpinski, J., Bianconi, A.: *Phys. Rev. B* **82**, 144507 (2010)
- Ricci, A., Joseph, B., Poccia, N., Xu, W., Chen, D., Chu, W.S., Wu, Z.Y., Marcelli, A., Saini, N.L., Bianconi, A.: *Supercond. Sci. Technol.* **23**, 052003 (2010)
- Dai, X., Le, C.-C., Wu, X.-X., Hu, J.-P.: *Chin. Phys. B* **25**, 077402 (2016)
- Hulliger, J., Awan, M.A.: *J. Comb. Chem.* **7**, 73 (2005)

21. Iranmanesh, M., Stir, M., Kirtley, J.R., Hulliger, J.: *Chem. Eur. J.* **20**, 15816 (2014)
22. Hiroi, Z., Takano, M., Azuma, M., Takeda, Y.: *Nature* **364**, 315 (1993)
23. Shaked, H., Shimakawa, Y., Hunter, B.A., Hitterman, R.L., Jorgensen, J.D., Han, P.D., Payne, D.A.: *Phys. Rev. B* **51**, 11784 (1995)
24. Azuma, M., Hiroi, Z., Takano, M., Bando, Y., Takeda, Y.: *Nature* **356**, 775 (1992)
25. Kawashima, T., Takayama-Muromachi, E.: *Physica C* **267**, 106 (1996)
26. Jin, C.-Q., Adachi, S., Wu, X.-J., Yamauchi, H., Tanaka, S.: *Physica C* **223**, 238 (1994)
27. Pérez, D., Hulliger, J.: *Rev. Sci. Instrum.* **81**, 065108 (2010)
28. Tamura, T., Adachi, S., Wu, X.-J., Tatsuki, T., Tanabe, K.: *Physica C* **277**, 1 (1997)
29. Liu, J., Li, F.H., Wan, Z.H., Fan, H.F., Wu, X.J., Tamura, T., Tanabe, K.: *Mater. Transc.* **39**, 920 (1998)
30. Wu, X.-J., Tamura, T., Adachi, S., Tatsuki, T., Tanabe, K.: *Physica C* **299**, 249 (1998)
31. Rouillon, T., Provost, J., Hervieu, M., Groult, D., Michel, C., Raveau, B.: *Physica C* **159**, 201 (1989)